

Effects of Reducing Wind-Induced Trajectory Uncertainty on Sector Demand

Alfonso Valenzuela, Antonio Franco, and Damián Rivas
Department of Aerospace Engineering
Universidad de Sevilla, 41092 Seville, Spain
Email: avalenzuela@us.es

Javier García-Heras and Manuel Soler
Department of Bioengineering and Aerospace Engineering
Universidad Carlos III de Madrid, 28911 Leganés, Spain

Abstract—In this paper, a first step to analyse the effects of reducing the uncertainty of aircraft trajectories on sector demand is presented. The source of uncertainty is wind, forecasted by Ensemble Prediction Systems, which are composed of different possible atmosphere realizations. A trajectory predictor determines the routes to be followed by the different flights to reduce the uncertainty of the arrival times. The sector demand is described in terms of entry count, that is, the number of flights entering the sector during a selected time period, which is uncertain because so are the the entry times to the sector. Results are presented for a realistic application, where the dispersion of the entry count is shown to be reduced when the dispersion of the arrival times is also reduced.

I. INTRODUCTION

In 2005, the European Commission stated the political vision and high level goals for the Single European Sky and its technological pillar SESAR. Accomplishing the goals of increasing capacity and improving safety requires a paradigm shift in operations through state-of-the-art, innovative technology and research. A promising approach that can improve current prediction and optimization mechanisms towards meeting these goals is to model, analyse, and manage the uncertainty present in Air Traffic Management (ATM).

Weather uncertainty is one of the main sources of uncertainty that affect the ATM system [1]. The limited knowledge about present and, especially, future meteorology conditions, such as wind velocity and direction, fog, snowfall or storms, is responsible for much of the delays and flight cancellations, which negatively affects ATM efficiency and translates to extra costs for airlines and air navigation service providers.

The work presented in this paper shows that the effects of wind uncertainty on the prediction of the demand of an Air Traffic Control (ATC) sector can be reduced when the airspace users plan the route of each individual flight with the objective of increased predictability. The general framework of this work is the project TBO-Met¹, funded by the SESAR Joint Undertaking. The overall objective of this project is threefold: 1) to advance in the understanding of the effects of meteorological uncertainty in Trajectory-Based Operations (TBO), 2) to develop methodologies to quantify and reduce the effects of meteorological uncertainty in TBO, and 3) to

pave the road for a future integration of the management of meteorological uncertainty into the ATM system.

Ensemble Weather Forecasting is a prediction technique that allows to estimate the uncertainty in a weather forecast. In this work, the meteorological uncertainty is provided by Ensemble Prediction Systems (EPS). Typically, an EPS is a collection of 10 to 50 forecasts, referred to as members, with forecasting horizons of up to 2-5 days. They consist on running many times a deterministic model from very slightly different initial conditions [2]. Often, the model physics is also slightly perturbed, and some ensembles use more than one model within the ensemble or the same model but with different combinations of physical parameterization schemes. This technique generates a representative sample of the possible realizations of the potential weather outcome. The uncertainty information is on the spread of the solutions in the ensemble, and the hope is that the spread of the predictions in the ensemble brackets the true weather outcome [3].

Uncertain trajectories are obtained during the process of trajectory planning when meteorological uncertainty is taken into account. For each flight, the trajectory predictor computes an ensemble of aircraft trajectories, each one corresponding to a different member of the EPS [4]. Because they are computed for different weather realizations, different flight durations and fuel consumptions are obtained [5]. For each flight, the trajectory predictor developed in TBO-Met [6] determines an optimised route, which minimises a combination of the average and the dispersion of the flight time. The relative importance of each term can be adjusted through a parameter to make the trajectory more or less predictable. The trajectories of all flights, along with the information of the ATC sector, are then used to analyse the sector demand.

In this work, the sector demand is described in terms of the entry count, which is defined as the number of flights entering the ATC sector during a selected time period [7]. This count is obtained from the intersections of the individual aircraft trajectories with the boundary of the sector. Since the aircraft trajectories are uncertain, then the associated entry times are also uncertain and, thus, the entry count is also uncertain. The analysis is then based on the statistical characterization of these times and this count [8].

Results are presented for a realistic application. The demand of an ATC sector is analysed for a whole day when predicted

¹<https://tbomet-h2020.com/>

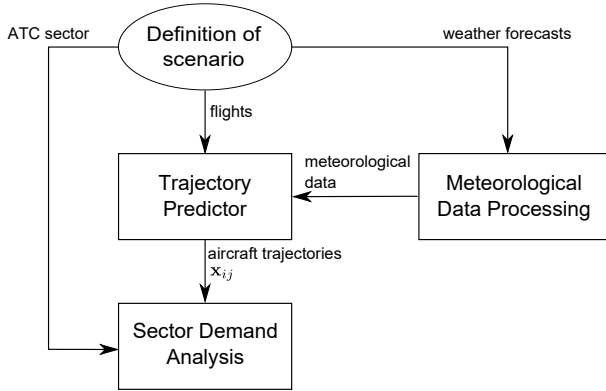


Figure 1. General scheme for the analysis of sector demand.

the day before, as would do, for example, the Network Manager when balancing capacity and demand. In this application, it is shown the effect of increasing the predictability of the individual flights on the entry times and the entry count.

II. METHODOLOGY FOR SECTOR DEMAND ANALYSIS

The general scheme for the analysis of sector demand is shown in Figure 1, see Ref. [8]. Initially, a scenario is defined in terms of: 1) ATC sector (e.g., geometry and capacity), 2) flights that cross the sector (e.g., origin and destination, departure times, flight levels, and cruise speeds), and 3) weather forecasts (e.g., EPS to be considered, release time, and forecast times).

The meteorological data provided by weather forecasts need to be processed for its use by the trajectory predictor. For example, the necessary values of wind and air temperature are extracted, and information about convection can be derived from different parameters.

The trajectory predictor computes, for each flight and for each weather prediction, a different aircraft trajectory. The trajectory predictor used in this application and developed in TBO-Met is described in Section III. The computed trajectories, along with the information of the ATC sector, are then used to perform the analysis of the sector demand. The different atmospheric realizations lead to different predicted entry times and, therefore, to different entry counts. In this work, this trajectory predictor is adjusted to obtain more predictable trajectories.

To perform the analysis of the sector demand, the entry times of the flights to the sector and the entry count are statistically characterized. Mean, maximum, and minimum values, and the spread of the times and of the count, measured as the difference between the maximum and minimum values, are examined.

A. Definitions and general hypotheses

In this work, it is considered that the geometry of the ATC sector is fixed and does not change with time. Therefore, the effects of opening/closing sectors are not analysed.

It is considered that there exist m different flights and that the EPS is formed by n different members or atmospheric

realizations. The position of flight i ($i = 1, \dots, m$) for member j ($j = 1, \dots, n$) at time t , is denoted as $\mathbf{x}_{ij}(t)$. It is given by the longitude λ , the latitude ϕ , and the pressure altitude h :

$$\mathbf{x}_{ij}(t) = [\lambda_{ij}(t), \phi_{ij}(t), h_{ij}(t)] \quad (1)$$

The trajectories \mathbf{x}_{ij} generated by the trajectory predictor are provided as a list of discrete points and times. A linear interpolation is used to obtain the position of the aircraft at any time.

In this work, it is considered that the trajectory crosses the ATC sector only once; trajectories that cross the same sector multiple times are not considered (for example, flights that return to the departure airport), because this is an uncommon practice in commercial aviation.

B. Entry time and entry distance

If the trajectory \mathbf{x}_{ij} crosses the ATC sector, then there exist an entry time to the sector $t_{ij,E}$ and the associated entry point $\mathbf{x}_{ij}(t_{ij,E})$. In this work, since the considered trajectory predictor determines a unique route for all the weather realizations, the entry point is the same for all the members of the EPS. The uncertainty information is on the spread of the entry times.

The entry times are statistically characterized. For flight i , we define the average entry time $t_{i,E}$ as

$$t_{i,E} = \frac{1}{n} \sum_{j=1}^n t_{ij,E} \quad (2)$$

and the dispersion of the entry time, $\Delta t_{i,E}$, as the difference between the maximum and the minimum values for the different atmospheric realizations

$$\Delta t_{i,E} = \max_j t_{ij,E} - \min_j t_{ij,E} \quad (3)$$

For flight i , the entry distance is the distance travelled by the aircraft from its origin to the entry point, denoted as $d_{i,E}$. Since the trajectories will be provided as a list of discrete points, the distance between two consecutive points is calculated considering a rhumb line.

C. Entry count

The entry count for a given sector is defined as the number of flights entering the sector during a selected time period P_k . In this paper, time periods with durations $\delta t = 10, 30$, and 60 minutes are considered.

Because the entry times are uncertain, the aircraft may enter the sector in different time periods, thus leading to an uncertain entry count. The larger the dispersions of the entry times and the smaller the values of δt , the more likely the entry count to be uncertain. For example, in case that the dispersion of the entry time of one flight is larger than the duration of the time period, then this flight may enter the sector in two or more consecutive time periods.

An entry function for flight i , for ensemble member j , and for time period P_k is defined, denoted as $E_{ij}(P_k)$: it takes the

value 1 when the aircraft enters the ATC sector during this time period and the value 0 otherwise

$$E_{ij}(P_k) = \begin{cases} 1 & \text{if } t_{ij,E} \in P_k \\ 0 & \text{if } t_{ij,E} \notin P_k \end{cases} \quad (4)$$

The entry count for ensemble member j and for time period P_k , denoted as $E_j(P_k)$, is obtained as the sum of the entries of the different flights

$$E_j(P_k) = \sum_{i=1}^m E_{ij}(P_k) \quad (5)$$

From these n values of the entry count, mean, maximum, and minimum values (\bar{E} , E_{\max} , and E_{\min} , respectively) for time period P_k are determined

$$\bar{E}(P_k) = \frac{1}{n} \sum_{j=1}^n E_j(P_k) \quad (6)$$

$$E_{\max}(P_k) = \max_j E_j(P_k) \quad (7)$$

$$E_{\min}(P_k) = \min_j E_j(P_k) \quad (8)$$

The uncertainty information is on the spread of the entry count. The dispersion of the entry count, $\Delta E(P_k)$, is defined as follows

$$\Delta E(P_k) = E_{\max}(P_k) - E_{\min}(P_k) \quad (9)$$

Notice that, since the entry of each flight to the ATC sector for time period P_k only depends on the entry time $t_{ij,E}$, see Eq. (4), then the entry count and its statistical characterization are only affected by the uncertainty in this time. Therefore, the uncertainty in the entry count increases when the uncertainty in the entry time increases.

III. TRAJECTORY PREDICTOR

The trajectory predictor considered in this work solves the problem of trajectory planning considering uncertain wind fields provided by EPS, see Ref. [6]. For each flight and a given EPS formed by n members, the trajectory predictor determines n different trajectories, each one corresponding to a different ensemble member. All trajectories follow the same route, described as a sequence of waypoints. The difference between the trajectories is then the arrival times to the waypoints of the route, because they are subject to different wind fields. Since each member of the forecast is considered as equally probable, then each trajectory is also considered as equally probable.

The route determined by the trajectory predictor for each flight minimises a weighted sum of the average flight time of the n trajectories and of the flight-time dispersion, measured as the difference between the maximum flight time $t_{f,\max}$ and the minimum flight time $t_{f,\min}$. The relative weight of the dispersion is controlled by a parameter denoted as p . By changing the value of this parameter, one can obtain routes that are more efficient on average (they arrive earlier) or routes that are more predictable (they show less dispersion).

In this work, the en-route phase is considered, flown at constant altitude and constant airspeed. The inclusion of variable altitude and speed profiles, and the exploration of other objective functions that include the flight dispersion is left for future work, see for instance Ref. [9].

This problem of trajectory planning is formulated as a deterministic optimal control problem, where the n trajectories are simultaneously considered. For each flight, the mathematical formulation of the problem is as follows

$$\min \frac{1}{n} \sum_{j=1}^n t_j(r_f) + p(t_{f,\max} - t_{f,\min}) \quad (10)$$

subject to the constraints

$$\frac{d}{dr} \begin{bmatrix} \phi \\ \lambda \\ t_1 \\ \vdots \\ t_n \end{bmatrix} = \begin{bmatrix} \frac{\cos(\chi_g)}{R_E + h} \\ \frac{\sin(\chi_g)}{(R_E + h) \cos \phi} \\ \frac{1}{V_{g,1}} \\ \vdots \\ \frac{1}{V_{g,n}} \end{bmatrix} \quad (11)$$

$$\begin{bmatrix} V_{g,1} \cos(\chi_g) \\ \vdots \\ V_{g,n} \cos(\chi_g) \\ V_{g,1} \sin(\chi_g) \\ \vdots \\ V_{g,n} \sin(\chi_g) \end{bmatrix} = \begin{bmatrix} V \cos(\chi_1) + w_{y,1}(\phi, \lambda) \\ \vdots \\ V \cos(\chi_n) + w_{y,n}(\phi, \lambda) \\ V \sin(\chi_1) + w_{x,1}(\phi, \lambda) \\ \vdots \\ V \sin(\chi_n) + w_{x,n}(\phi, \lambda) \end{bmatrix} \quad (12)$$

where r is the distance flown along the route, r_f is the distance flown when arriving to the destination, $t_j(r)$ is the flight time at distance r for ensemble member j , χ_g is the course, $R_E = 6371$ km is the Earth radius considered as a sphere, $V_{g,j}$ are the groundspeeds derived from the winds provided by the ensemble member j , V is the aerodynamic airspeed, χ_j is the heading for ensemble member j , and $w_{x,j}$ and $w_{y,j}$ are the zonal and meridional components of the wind for member j . Notice that the wind does not depend on the time in this formulation, it is obtained from the forecast closer to the middle time of the flight. An estimation of the arrival time needs to be provided to choose the appropriate forecast beforehand.

The boundary conditions of the problem are

$$\begin{aligned} (\phi(0), \lambda(0)) &= (\phi_0, \lambda_0) \\ (\phi(r_f), \lambda(r_f)) &= (\phi_f, \lambda_f) \\ t_j(0) &= t_0, \quad \forall j \in \{1, \dots, n\} \end{aligned} \quad (13)$$

where ϕ_0 and λ_0 are the coordinates of the departure point, ϕ_f and λ_f are the coordinates of the destination point, and t_0 is the departure time.

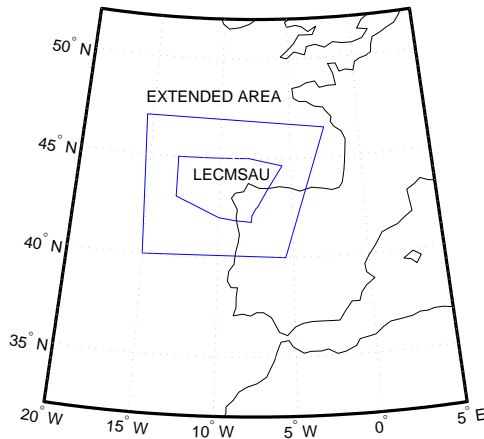


Figure 2. Geographical location of ATC sector LECMSAU and the extended area.

The resolution of this mathematical problem relies on an initialization and wind approximation procedure described in Ref. [10]. It is solved with direct methods, discretizing the trajectory with a trapezoidal scheme and then solving the resulting nonlinear optimization problem with NLP software (see, for example, Ref. [11]).

IV. APPLICATION

In this application, the demand of the ATC sector LECMSAU is analysed for a whole day, 01 September 2016 (from 00:00 to 24:00), when predicted the day before, 31 August at 00:00. Next, the traffic scenario is described, in terms of ATC sector, flights, and weather forecasts. The results are presented and analysed in Section V for two different values of the parameter p .

A. ATC sector

The sector LECMSAU is located in the Northwest of Spain, see Figure 2. It is an en-route sector, ranging from flight level 345 to 460. Its declared capacity (i.e., the maximum number of flights entering the sector per hour) is 36 flights/hour. This information has been obtained from Eurocontrol's Network Strategic Tool (NEST) for the Aeronautical Information Regulation and Control (AIRAC) cycle 1609.

B. Flights

The information of the flights is also obtained from NEST, and it corresponds to the last filed flight plans from the airlines (i.e., initial trajectories, according to NEST nomenclature). Notice that the optimal routes determined by the trajectory predictor of this work are, in general, different from the routes filed in the flight plans, and it may happen that an optimal route crosses the sector whereas the corresponding planned route does not. Therefore, to take into account this situation, it has been decided to consider flights that planned to cross an extended area around LECMSAU. The coordinates of the four

vertices of this area are (see Figure 2): (N 47°, W 15° 30'), (N 46° 30', W 2° 30'), (N 40°, W 5° 30'), (N 40°, W 15°).

A total number of 1443 flights is obtained from NEST for the date of analysis and the extended area. However, 51 of these flights are discarded, those flights arriving or departing to/from LEST, LEVX, and LECO airports. The reason is that, under the hypothesis of flying at constant pressure altitude, these flights instantly appear or disappear inside the sector, not crossing the sector boundaries. Thus, a total number of 1392 flights is considered in this application. This traffic is composed of short flights (departing from Portugal, Spain, and France), medium flights (flights from the Canary Islands, the British Isles, the Scandinavian Peninsula, and Eastern Europe), and long flights (from South, Central, and North America).

The trajectory predictor described in Section III requires the following information for each flight:

- coordinates of the departure and arrival airports: obtained from NEST;
- departure time: obtained from NEST;
- arrival time: obtained from NEST, used as a reference time;
- pressure altitude: fixed to 200 hPa (approximately 38600 ft) for all aircraft and the whole flight;
- airspeed: the average cruise Mach provided by Eurocontrol's Base of Aircraft Data (BADA) 3.13 [12] for the aircraft model that performs the flight is considered for the whole flight (from origin to destination), ranging from 0.63 to 0.85.

C. Weather forecast

The meteorological uncertainty is retrieved from the European Centre for Medium-Range Weather Forecasts. In particular, the weather forecast ECMWF-EPS, composed of 50 perturbed members, is used.

Since the analysis is performed the day before the operation, the forecasts released at 00:00 on 31 August 2016 are considered. According to the flight plans retrieved from NEST, the earliest flight departs at 16:20 on 31 August and, as a reference, the latest flight arrives to its destination at 09:54 on 02 September. Taking into account these times, the forecasts with forecasting horizons of 12, 18, 24, 30, 36, 42, 48, 54, and 60 hours are considered.

In agreement with the coordinates of the route waypoints, the forecasts are retrieved for a coverage area which ranges from 45 degrees South to 75 degrees North, and from 130 degrees West to 50 degrees East. The spatial grid resolution is 0.25 degrees. According to the cruise altitude chosen for all flights, the forecasts are retrieved for the pressure level 200 hPa.

The meteorological variables required by the trajectory predictor described in Section 3.2 are the zonal wind and the meridional wind (winds along the West-East and South-North directions, respectively).

In Figures 3 and 4, the average and the dispersion of the meridional and the zonal winds are shown for the forecast corresponding to the time instant 12:00 on 01 September. The

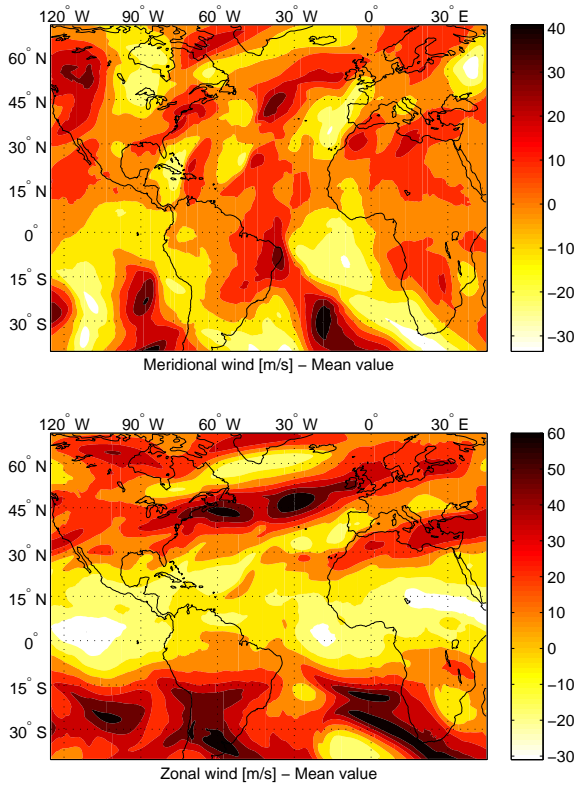


Figure 3. Average meridional (top) and zonal (bottom) winds, ECMWF-EPS released at 00:00, 31/08/16, forecasting horizon 36 hours.

dispersion is measured as the difference between the maximum and the minimum values at each geographic location.

The average meridional wind, see Figure 3 top, ranges approximately between -30 m/s (South direction) and 40 m/s (North direction). High values of the wind are found at the East coast of North America and the North Atlantic Ocean. The average zonal wind, see Figure 3 bottom, is larger than the meridional wind, ranging approximately between -30 m/s (West direction) and 70 m/s (East direction). The zonal wind is therefore the main contributor to the existence of jet streams. The larger values are found again at the East coast of North America, the North Atlantic Ocean, and South America.

The dispersion of the winds, see Figure 4, is rather large, with maximum values above 40 m/s. The geographic areas affected by high uncertainty are approximately the same in both cases. In particular, it can be highlighted the East coast of North America and the North Atlantic Ocean, affecting flights from North America to Europe.

V. RESULTS

Next, results are presented for two different values of the relative weight of the dispersion, $p = 0$ and $p = 20$. Notice that, for a given flight and for each value of the parameter p , a different route is obtained which may or may not cross the sector. Trajectories that exit the sector and briefly enter again have been discarded for being not realistic.

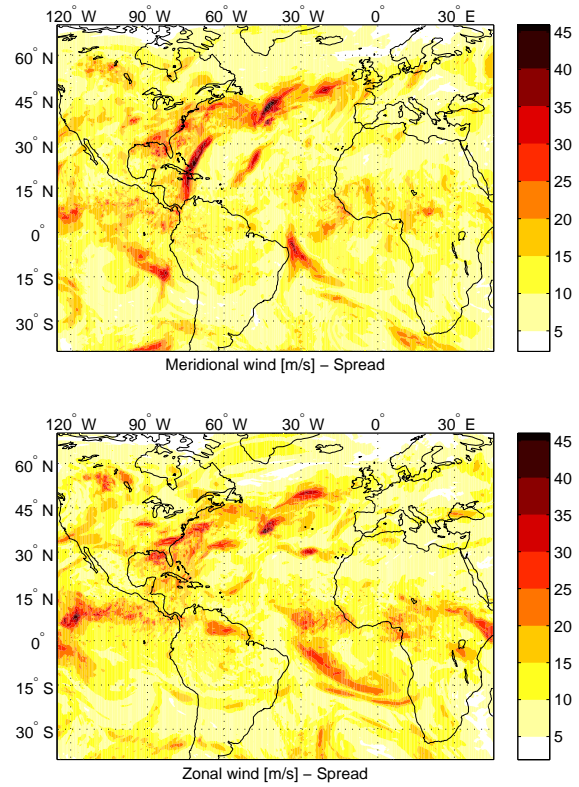


Figure 4. Dispersion of the meridional (top) and zonal (bottom) winds, ECMWF-EPS released at 00:00, 31/08/16, forecasting horizon 36 hours.

The number of trajectories that enter the sector for $p = 0$ is 440 and for $p = 20$ is 624. In this work, only the effect of the reduction of the time dispersion on the sector demand is analysed. For this reason, 328 flights are considered, those flights that cross the sector LECMSAU for both values of p . The effect of the varying number of aircraft entering the sector, that is, the displacement of the traffic flows from one sector to another, is left for future work.

A. Entry times

The dispersion of the entry time, $\Delta t_{i,E}$, as a function of the distance to the entry point, $d_{i,E}$, for each flight is presented in Figure 5. Firstly, one can see that, as one could expect, in general the dispersion increases as the distance increases because the uncertainty is accumulated along the trajectories; flights arriving from distant locations present more uncertainty. For example, for $p = 0$, the maximum dispersion is as large as 449 seconds and it is found for 7553 km.

Secondly, it can be seen that there are flights with similar distances but different values of dispersion. For example, for $p = 0$ and for $d_{i,E}$ approximately equal to 1500 km, the dispersion ranges between 115 and 339 seconds. As possible causes of these different values, the following ones can be highlighted:

- different routes (flights over regions of the airspace with different uncertainty),

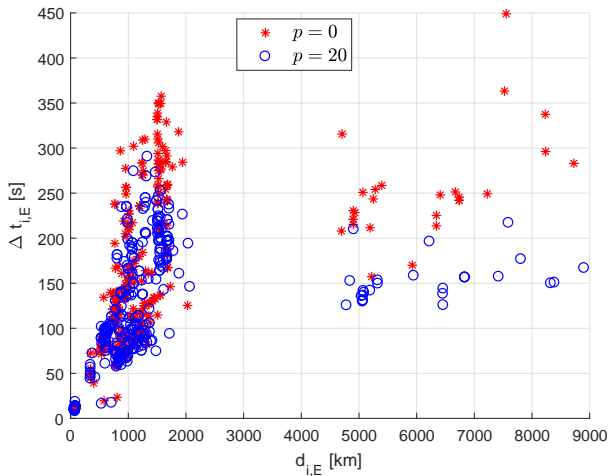


Figure 5. Dispersion of the entry time vs distance to the entry point.

- different effects of the same wind uncertainty on different flights (uncertainties in tail/headwinds have a higher impact than uncertainties in crosswinds),
- different departure times (the predictions for flights departing later are made with weather forecasts with larger time horizons, thus having a larger uncertainty), or
- different speeds (flights with lower values of Mach number and with headwinds are more sensitive to uncertainties in the wind).

Finally, it can be seen that the trajectories obtained for $p = 20$ show a lower dispersion in the entry time. The average value of dispersion for all the aircraft (that is, the average value of the points in Figure 5) is 156.4 s for $p = 0$, and 125.8 s for $p = 20$, a reduction of 30.6 s. However, as can be inferred from the objective function (10), this reduction of the dispersion comes from an increase of the average flight time. In this application, the average flight time increases 382.5 s.

B. Entry count

The entry count for $p = 0$ and three different time intervals, $\delta t = 60, 30,$ and 10 minutes, is shown in Figure 6. The average entry count is shown as vertical bars, and the minimum and maximum entry count as whiskers. The capacity of the sector is depicted as a red horizontal line, which is 36 flights/hour, and is assumed to be 18 flights/30 minutes, and 6 flights/10 minutes.

For the 60 minute interval, the largest value of the mean entry count is 40.5 flights, found at 07:00-08:00, which exceeds the sector capacity. The entry counts determined for smaller time intervals allow a more precise identification of the traffic peaks. In particular, for the 30 minute interval, the traffic peak takes the value 26.6 and is found in the period 07:00-07:30, and for the 10 minute interval it is 14.2 flights in 07:20-07:30, much higher than the assumed capacities.

The uncertainty on the entry count is on the spread of the number of flights, that is, the height of the whiskers in Figure 6, also represented in Figure 7 for convenience. For

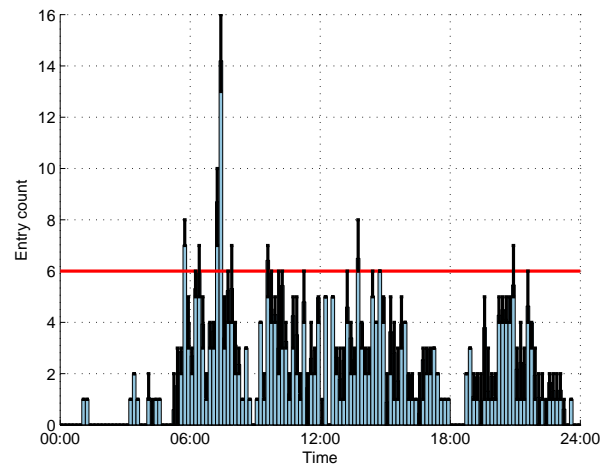
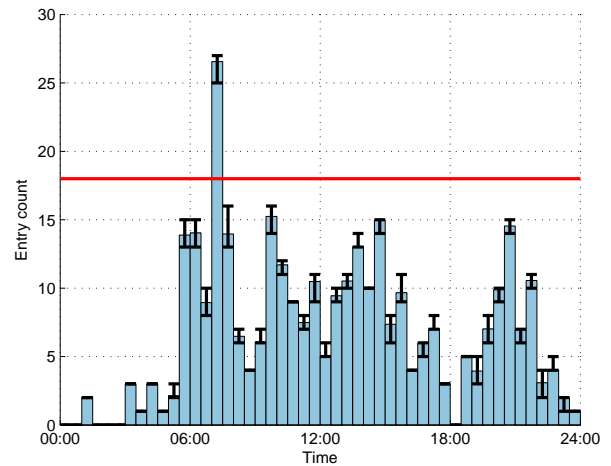
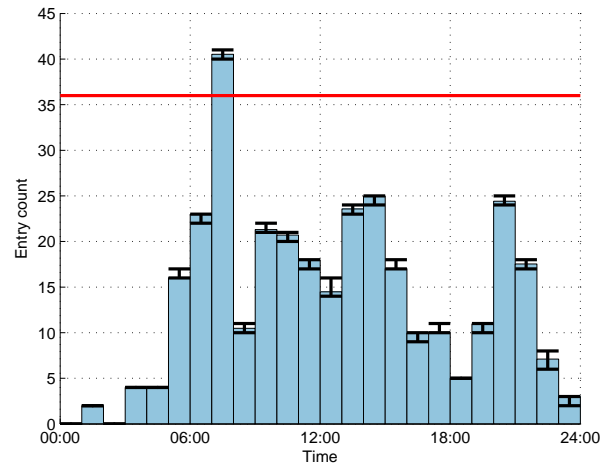


Figure 6. Entry count for $p = 0$ and $\delta t = 60$ minutes (top), 30 minutes (middle), and 10 minutes (bottom).

example, for $\delta t = 30$ minutes, the difference between the maximum and the minimum values of the entry count is as large as 3 flights for a total of 0.5 hours, 2 flights for 5.5 hours (in disjoint periods), 1 flight for 9 hours, and 0 flights for the remaining 9 hours.

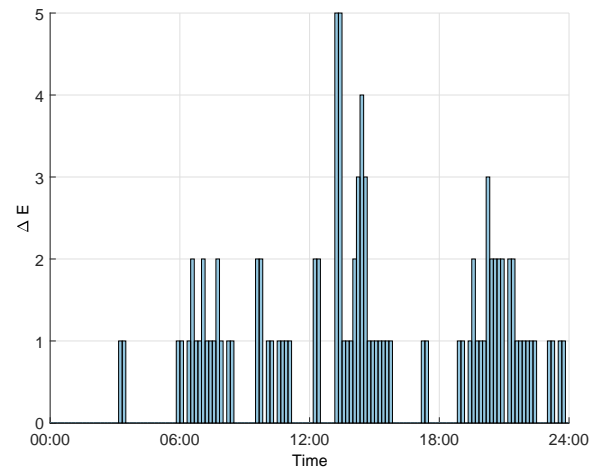
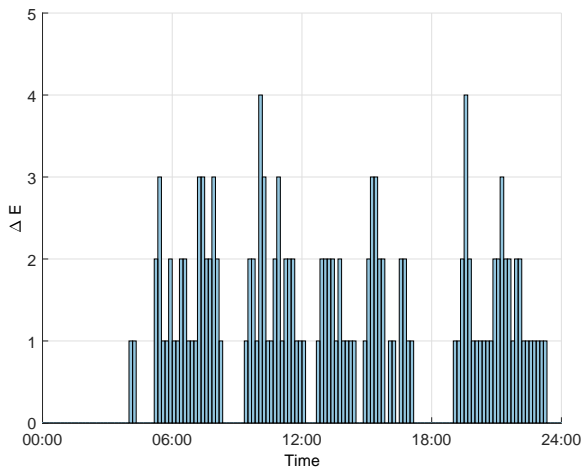
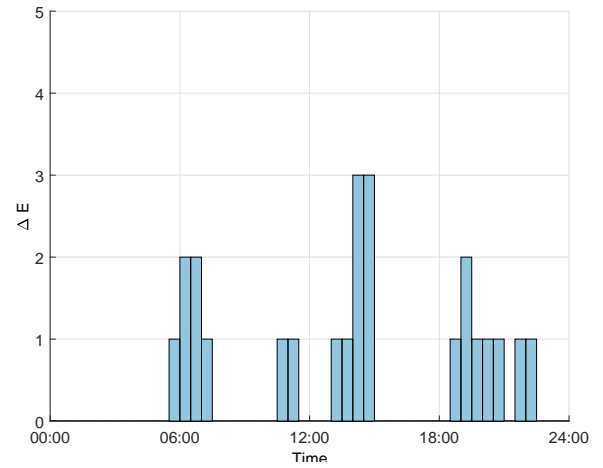
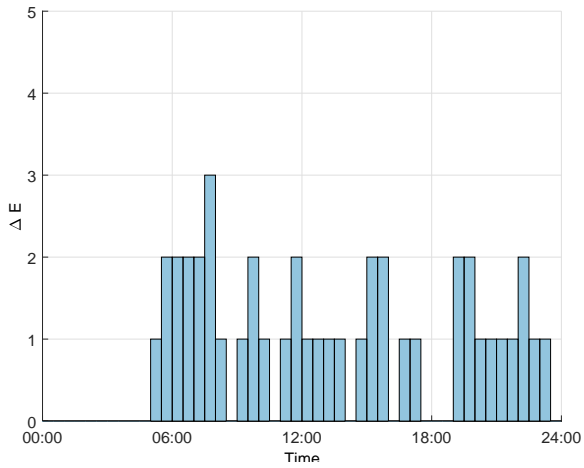
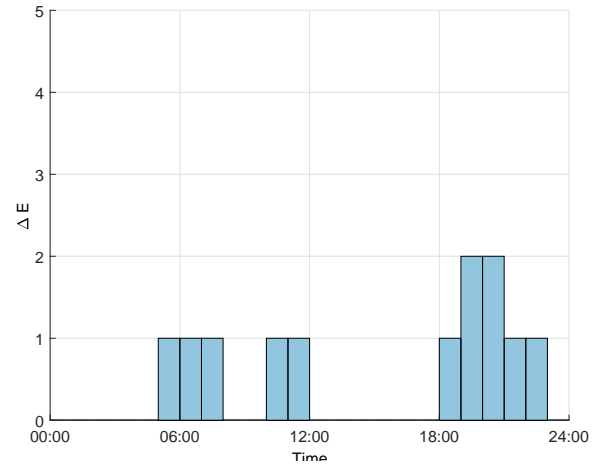
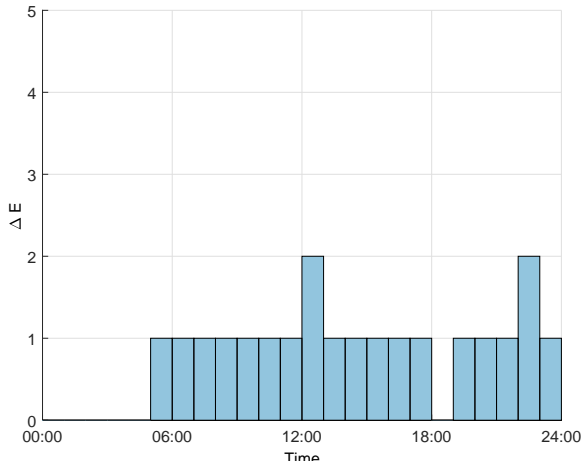


Figure 7. Dispersion of the entry count for $p = 0$ and $\delta t = 60$ minutes (top), 30 minutes (middle), and 10 minutes (bottom).

Figure 8. Dispersion of the entry count for $p = 20$ and $\delta t = 60$ minutes (top), 30 minutes (middle), and 10 minutes (bottom).

When the duration of the time periods is shortened, it can be observed that the maximum values of the dispersion increase, as already noted in Section II-C, but the average values of the entry counts are proportionally reduced; thus, the uncertainty becomes relatively more important. For example, for the 30 minute interval, the largest dispersion on the entry count is 3 flights and the average entry count is 6.83 flights/period (obtained as the number of flights entering the sector divided by the number of time periods), 44% in relative terms; whereas for the 10 minute interval the largest dispersion on the entry count is 4 flights and the average entry count is 2.28 flights/period, 175%.

For $p = 20$, the average entry counts are slightly different to those found for $p = 0$, shown in Figure 6, due to differences in the average entry times; they are not shown for brevity. The main difference between the two set of results is found in the dispersion of the entry count, as can be seen in Figure 8 compared to Figure 7. The maximum dispersion can be occasionally larger, for example, for 10 minutes and $p = 20$ the maximum dispersion is 5 flights, and for $p = 0$ is 4 flights, but on average, the dispersion is significantly reduced: for 60 minutes the average dispersion per period (and for the whole day) is reduced from 0.83 to 0.50 flights, for 30 minutes from 0.99 to 0.69, and for 10 minutes from 0.90 to 0.50.

VI. CONCLUSIONS

A first step to show the effects of reducing the uncertainty of aircraft trajectories on the sector demand has been presented in this paper. The source of uncertainty is wind, forecasted by Ensemble Prediction Systems. The uncertainty is reduced by a trajectory predictor to be employed by airspace users, which determines the appropriate route to minimise a weighted sum of the average flight time and of the flight-time dispersion. The sector demand is described by the entry count, which is uncertain because the entry times to the sector are uncertain.

In the application presented, it has been found that, because uncertainty is accumulated along the flight, the uncertainty in the entry time increases as the distance travelled by the aircraft to the entry point increases. Thus, sectors with predominance of incoming long-haul flights are expected to be more affected by weather uncertainty. Also, it has been found that the uncertainty in the entry count may be rather large, in particular when small time periods are considered. It is worth noting that, in this application, only wind uncertainties are considered. Larger values of uncertainty are expected in scenarios that consider uncertainties on air temperature and, primarily, convective phenomena.

When the dispersion of the individual trajectories is reduced, the dispersions of the entry times and of the entry counts are also reduced. However, this reduction of the dispersion comes from an increase of the average flight time and, thus, of fuel consumption and operating costs. Both the airlines and the Network Manager will benefit of better predictability. The airlines will know better when the aircraft will arrive to the destination airports, leading to a better fleet scheduling. The Network Manager will know more precisely the demand of

the sector, which may allow to improve the Demand-Capacity Balancing process, better identifying the Air Traffic Flow and Capacity Management measures to be applied.

It has been found that when the predictability of individual flights is increased, the trajectories are deviated, modifying the number of aircraft crossing the sector. The displacement of traffic flows from one sector to another is left for future work.

This analysis can be extended to consider other demand indicator as it is the occupancy count, that is, the number of flights inside the sector during a selected time period. For this count, it is necessary to consider also the exit time from the sector, which is also affected by the weather uncertainties that exist inside the ATC sector.

In the immediate future, under the scope of the TBO-Met project, this methodology will be applied to quantify the effects of weather uncertainty on convective phenomena. In this case, the uncertainty will be obtained from probabilistic nowcasts.

ACKNOWLEDGEMENTS

This work is part of the project TBO-Met. This project has received funding from the SESAR Joint Undertaking under grant agreement No 699294 under European Union's Horizon 2020 research and innovation programme.

REFERENCES

- [1] D. Rivas and R. Vazquez, "Uncertainty," in Complexity Science in Air Traffic Management, A. Cook and D. Rivas Ed., Ashgate Publishing Limited, 2016, Chap. 4.
- [2] World Meteorological Organization, "Guidelines on Ensemble Prediction Systems and Forecasting," WMO-No. 1091, 2012.
- [3] M. Steiner, R. Bateman, D. Megenhardt, Y. Liu, M. Xu, M. Pocernich and J. A. Krozel, "Translation of Ensemble Weather Forecasts into Probabilistic Air Traffic Capacity Impact," *Air Traffic Control Quarterly*, Vol. 18, No. 3, 2010, pp. 229–254.
- [4] J. Cheung, A. Hally, J. Heijstek, A. Marsman, and J.-L. Brenguier, "Recommendations on Trajectory Selection in Flight Planning based on Weather Uncertainty," Proc. 5th SESAR Innovation Days (SID2015), Bologna, Italy, 2015, pp. 1–8.
- [5] A. Franco, D. Rivas, and A. Valenzuela, "Optimal Aircraft Path Planning Considering Wind Uncertainty," Proc. 7th European Conference for Aeronautics and Space Sciences (EUCASS), Milan, Italy, 2017, pp. 1–11.
- [6] D. Gonzalez-Arribas, M. Soler, and M. Sanjurjo, "Wind-based Robust Trajectory Optimization using Meteorological Ensemble Probabilistic Forecasts," Proc. 6th SESAR Innovation Days (SID2016), Delft, Netherlands, 2016, pp. 1–8.
- [7] M. Dalichampt, and C. Plusquellec, "Hourly Entry Count versus Occupancy Count Definitions and Indicators (I)," EEC Note No. 15/07, Eurocontrol Experimental Centre, 2007, pp. 1–32.
- [8] A. Valenzuela, A. Franco, and D. Rivas, "Sector Demand Analysis under Meteorological Uncertainty," Proc. 7th European Conference for Aeronautics and Space Sciences (EUCASS), Milan, Italy, 2017, pp. 1–15.
- [9] D. González-Arribas, M. Soler, and M. Sanjurjo-Rivo, "Robust Aircraft Trajectory Planning Under Wind Uncertainty Using Optimal Control," *J. of Guidance, Control, and Dynamics*, published online, 16 October 2017.
- [10] D. González-Arribas, M. Soler, and M. Sanjurjo-Rivo, "Wind-Optimal Cruise Trajectories using Pseudospectral Methods and Ensemble Probabilistic Forecasts," Proc. 5th International Conference on Application and Theory of Automation in Command and Control Systems (ATACCS), Toulouse, France, pp. 160–167, 2015.
- [11] J. T. Betts, "Practical Methods for Optimal Control and Estimation using Nonlinear Programming," 2nd Edition, SIAM, 2010.
- [12] A. Nuic, "User Manual for the Base of Aircraft Data (BADA)," rev 3.13, 2015.